Mechanical and structural characteristics of commercially pure grade 2 Ti welds and solder joints

H. W. ANSELM WISKOTT, THIERRY DOUMAS, SUSANNE S. SCHERRER, URS C. BELSER
Division of Fixed Prosthodontics, University of Geneva, School of Dentistry, 19, rue Barthélemy-Menn, 1205 Geneva, Switzerland

CHRISTIAN SUSZ
Qualident Inc., Route des Acacias 14b, 1227 Acacias, Geneva, Switzerland
E-mail: anselm@wiskott.com

This study aimed at determining whether data previously gathered for a laser welds and IR brazings using a Au–Pd alloy were applicable to titanium joints. As to its resistance under fatigue loading, Au–Pd alloy had shown a poor response to pre-ceramic laser welding and post-ceramic brazing. The present study was designed to assess the mechanical resistance, the microstructure and the elemental diffusion of laser welded, electric arch welded and brazed joints using commercially pure titanium as substrate metal.

Mechanical resistance was determined by determining the joints' ultimate tensile strength and their resistance to fatigue loading. Elemental diffusion to and from the joints was assessed using microprobe tracings. Optical micrographs of the joints were also obtained and evaluated.

Under monotonic tensile stress, three groups emerged: (1) the GTAW and the native (i.e. as received) substrate, (2) the annealed substrate and the laser welds and (3) the brazed joints. Under fatigue stress, the order was: first the native and annealed substrate, second the brazings and laser welds, third the GTAW joints. No Au-filler brazing withstood the applied fatigue loading. The micrographs showed various patterns, an absence of HAZ cracking and several occurrences of Widmanstätten structures. Elemental diffusion to and from the Ti substrate was substantial in the Ti filler brazings and virtually nil in the Au-based brazings.

Under fatigue stress application, the titanium-based brazings as well as the laser- and electric arc welds performed equally well if not better than a previously tested AuPd alloy. There was a definite increase in grain size with increased heat application. However, no feature of the microstructures observed or the elemental analysis could be correlated with the specimen's resistance to fatigue stress application.

1. Introduction

Titanium, either commercially pure or alloyed, has been widely used as an orthopedic [1] and dental implant material [2]. Due to its surface chemistry, titanium represents a nearly perfect combination of tissue compatibility and mechanical resistance [3, 4]. To decrease the risks of corrosion between endosseous Ti implants and dental restorations exposed to the oral environment, it has been advocated to fabricate the superstructure frameworks out of titanium as well [5]. Such an approach often entails that Ti restorations be joined after casting using brazing or welding techniques.

In a previous study, we tested the mechanical resistance and microstructure of brazed joints and welds produced using a Au–Pd substrate alloy [6]. Two findings emerged: (1) The low-fusing brazing alloy (735–785 °C) was associated with high interfacial elemental diffusion and produced fairly low-strength joints. Conversely almost no diffusion was observed in the high-fusing (1000–1110 °C) brazings and the joints were among the strongest. (2) Under monotonic tensile stress, the laser welds' strength was close to the parent metal while their resistance to fatigue loading ranged among the lowest of the joints tested.

We also showed that laser welding produced highly dendritic structures and cracks in the HAZ of Au–Pd alloys [7]. It was hypothesized that the increased brittleness of such joints was the cause of the discrepancy observed between their high tensile strength under

monotonic force application and their low resistance to cyclic stresses. By contrast, the microstructure of high-fusing brazings was homogeneously granular and these joints were superior in their resistance to fatigue loading.

With some exceptions [8–10], the vast majority of information available on brazing and welding of titanium has been gathered using substrates and procedures relevant to industrial engineering (e.g. automated processes, high temperatures) [11]. It follows that commercially pure Ti (CpTi), whose mechanical resistance is comparatively low, has received less attention whereas Ti alloys – mostly Ti–6Al–4V but also other systems – have been investigated more extensively.

In clinical dentistry, laser and electric arc welding were essentially recommended for the joining of titanium structures, not for Au–Pd alloys as in our previous study. Due to a lack of information on CpTi, it was therefore unclear whether the findings reported previously applied to Au–Pd alloys only or should be extended to titanium substrates. The present investigation was thus undertaken to determine how titanium joints produced using a brazing technique, electric arc- and laser welding compared to data obtained for a Au–Pd dental alloy. Using grade 2 CpTi as substrate metal, the present investigation was designed to compare the mechanical properties, elemental diffusion and metallurgical structure of the joints thus produced.

2. Experimental

2.1. Substrate metal, brazing alloys

CpTi grade 2 titanium (ADS-Argen, Switzerland) [12] was used as substrate metal. Two filler alloys were tested, a titanium-based braze (Morita, Japan) and one gold-based (nickel-free) product (P3, Qualident, Switzerland). The chemical compositions of the substrate metal and the brazing alloys are detailed in Table I.

2.2. Welding and brazing procedures

Specimen preparation. 3.4 × 20 mm wire drawn rods were used. Post-machining grain structure was homogenized by annealing to 950 °C for 10 min [13]. Surfaces intended for laser welds were sandblasted using 50 μm AlO_3. Electric arc welding and brazing surfaces were sanded up to 1200 grit. The surfaces were further cleaned for 15 min in 3% solution of 80% HNO_3/20% HF to remove titanium oxides and hydrocarbon-embedded contaminants. Prior to joining, the specimens were rinsed in distilled water and acetone and dried with nitrogen gas. Welding was carried-out within 5 min after the cleaning procedures. After an initial round of preliminary tests conducted to optimize the settings of the brazing/welding devices used, the specimens were joined as follows.

Electric arc welding. This was performed using a 1.5 KW GTAW device developed for dental applications (OAW-2OUS, O'Hara, Japan). The shielding gas was argon. Both rods were positioned in a jig to set a joint clearance of 0.2 mm. A 1 mm strip of CpTi grade 2 was used as filler metal. The device was operated at current intensities in the 15–20A range.

Laser welding. For laser welding, a Nd : YAG device (DL 2000, Dentaurum, Germany) was operated at 280 V with 0.6 ms pulses (0.74 J). Oxide formation was prevented by argon flushes that preceded beam activation. During welding, the rods were clamped in a V-shaped jig which was held by the operator who could monitor their orientation through an ancillary binocular. By rotating the jig, the operator established a continuous weld seam along the mating surfaces.

Brazing. This was carried out with an argon-protected IR heating oven (R-S-1, Morita, Japan) [14]. The filler metals were flown into gaps set to 0.2 mm. Due to deficiencies in the power of the instrument, the rods had to be clamped in a machined ceramic jig to decrease thermal inertia. An argon atmosphere was maintained during the entire joining process to prevent oxidation. Melting of the filler metal was ascertained visually through the quartz window of the device. After joining, the specimens were oven-cooled to room temperature (no quenching).

2.3. Mechanical strength testing

Specimen preparation. All specimens were slightly angled after joining. To re-establish a coaxial arrangement of the rods for testing, the specimens were machined using a precision centerless grinding machine (Model 150-SL 20, Agathon, Switzerland). After truing the specimens, the samples were spun on a lathe and the joints' surfaces were refined up to 1000 grit silicon paper. Then the specimens were ultrasonically cleaned and inspected under 20 × magnification. All solder joints with surface defects were eliminated. Small voids in laser welds were corrected by additional welding.

The specimens intended for fatigue tests were left as cylinders (Fig. 1A). The specimens for tensile tests were first waisted and a flat was ground into the specimens. Then, while stabilizing the specimens with a hex wrench, a thread was cut into both ends of the rods (Fig. 1B).

The substrate metal specimens for fatigue tests were

TABLE I Composition of the substrate alloy and filler metals (wt %)

Cp titanium grade 2*	N	C	H	Fe	O	Ti	Melting point
	0.03	0.10	0.015	0.30	0.25	balance	1667 °C
TiCuNi (filler metal)	Ti	Cu	Ni				Melting range
	60	15	25				902–932 °C
P3 (filler metal)	Au	Pt	Ag	Zn			Melting range
	80	7.5	10.5	2			995–1070 °C

*Maximum (given the tolerances of ASTM F 67–83).

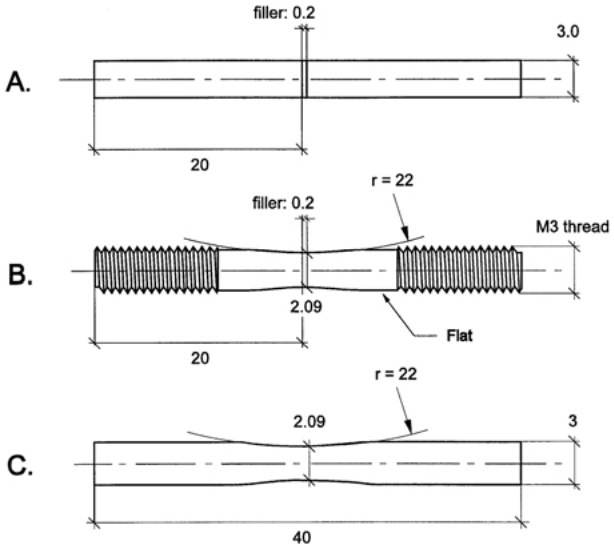

Figure 1 Specifications of specimens after truing. When filler metal was used (brazings and GTAW), the clearance provided was 0.2 mm. A. Specimens for fatigue tests. B. Specimens for tensile tests. C. Specimens for substrate metal fatigue tests.

annealed and milled to a waisted shape (Fig. 1C) [15]. Tensile specimens were further threaded on both ends (Fig. 1B). Prior to testing, all joined specimens were run through a heating schedule intended to duplicate the temperature cycles during firing of the ceramic veneer. The samples were thus heated to 830, 755, 745, 735 and 690 °C with a 1 min dwell time at maximum temperature. All specimens were oven cooled.

Ultimate tensile strength (UTS). The samples $(n = 10)$ were tested for UTS using a universal testing machine. The threaded portions of the rods were screwed into appropriate keyway parts which were fastened to the beams of the testing machine *via* self aligning gripping devices. The cross-head speed was set to 0.3 mm per minute.

Fatigue resistance. Resistance to fatigue stresses was determined using an experimental set-up described previously [16, 17]. In essence, the procedure relies on incremental loading of the soldered specimens $(n = 30)$ mounted as rotating cantilever beams $(R = -1)$. The stress induced in the joint (σ) being calculated as [18]:

$$\alpha = F \frac{l}{\pi \frac{d^3}{32}}$$

where F is the force applied, l is the lever length and d the diameter of the joint. The specimens were processed according to the staircase method, a technique that yields a mean force $\pm$ SD at which 50% of the specimens fail and 50% survive a predetermined number of cycles. The details of the numerical treatment have been described elsewhere [19, 20]. The parameters set for the procedure were: entry level for staircase analysis: 250 MPa, in/decrement: 25 MPa, cycling speed: 1000 rpm (16.7 Hz), censoring at 10^6 cycles. 30 valid runs were required for each joint tested.

2.4. Microstructure

Joint interface regions were examined by optical microscopy. Surfaces were prepared for metallography by wet abrasion with sand papers up to 4000 grit. They were then polished with 3 and 1 µm diamond pastes at 150 rpm/1.5 N for 2 min. The surfaces were lubricated with a solution of alcohol and H_2O_2. To prevent any pollution between abrasives, the surfaces were washed with propyl alcohol. No glycerin was added to the abrasive slurry. High-gloss was obtained after polishing with a mixture of 96 ml oxides suspension (OP-S, Struers, Denmark), 2 ml 30% H_2O_2 and 2 ml 32% ammonia. Finally, the specimens were patterned by dipping the samples for 20 s into an acid mixture of 135 ml water, 5 ml 60% HNO_3 and 10 ml 40% HF. After drying, the surfaces were photographed using an inverted microscope (Diavert, Leitz, Germany).

2.5. Elemental diffusion

The soldered/welded specimens were first embedded into an electrically conducting compound and ground to expose the joints. Surfaces were prepared for analysis by following the same protocol as for optical metallography. Diffusion analysis was conducted using a SX-50 electron microprobe (Cameca, France). The settings of the device were as follows: voltage: 20 kV; electron beam: 30 nA. After calibration of the instrument, two metallurgically prepared specimens were placed into the vacuum chamber of the probe and the beam was run twice across each joint.

2.6. Microhardness

Microhardness was recorded with an automated micro-indenter (HMV-20, Shimadzu, Japan) operated at a load of 1 N which recorded the dimensions of the indentation and calculated the corresponding Vickers hardness.

3. Results

Ultimate tensile strength. Fig. 2 shows the UTS of the six groups. Statistically (ANOVA, $p < 0.5$), four groups emerged: (1) the electric arch welds with an UTS of 562 $\pm$ 22 MPa (mean $\pm$ SD) and the native (i.e. unannealed) substrate metal (555 $\pm$ 3 MPa). (2) the annealed substrate (499 $\pm$ 6 MPa) and the laser welds (488 $\pm$ 23 MPa); (3) the TiCuNi brazed joints

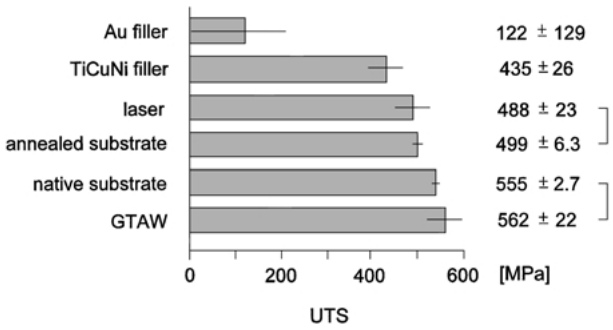

Figure 2 UTS of joints tested. Brackets indicate the absence of statistically significant difference $(p < 0.05)$. Native substrate = as received.

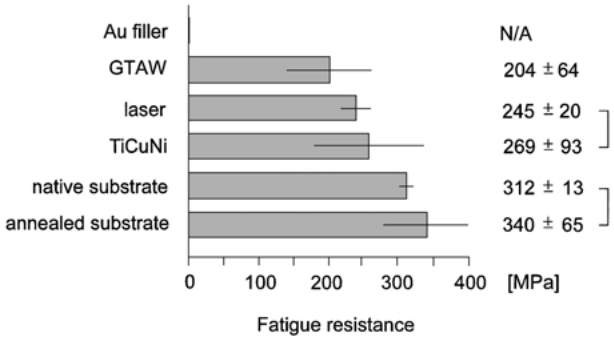

Figure 3 Fatigue resistance of joints tested. Brackets indicate the absence of statistically significant difference ($p < 0.05$). ''Native substrate'' = as received substrate metal.

(435 ± 26 MPa) and (4) the joints produced using the gold-based filler alloy (122 ± 129 MPa).

Resistance to cyclic loading. Fatigue resistance is depicted in Fig. 3. In decreasing order of strength, the annealed substrate metal came first with 340 ± 65 MPa (mean ± 95% CI) followed by the native substrate (312 ± 13 MPa), the TiCuNi brazed joints (269 ± 93 MPa), the laser welds (245 ± 20 MPa) and the GATW joints (204 ± 64 MPa). For all practical purposes, no fatigue resistance value could be ascribed to the gold brazed joints since even at the initial increment (25 MPa), none of the specimens reached 10^6 load cycles.

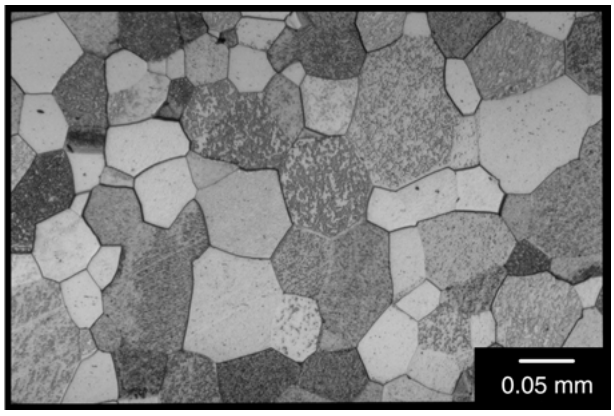

Figure 4 Annealed substrate. Equiaxed α grains (× 200).

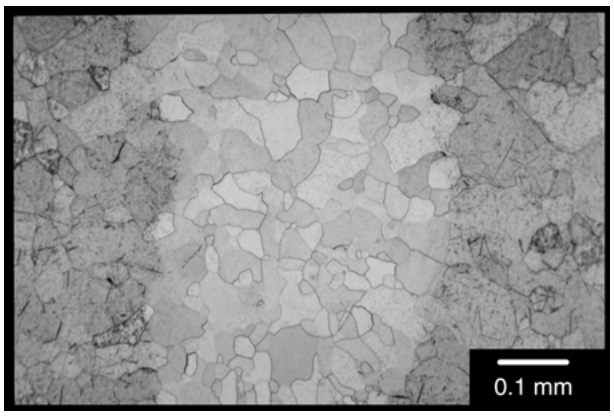

Figure 5 Laser weld. HAZ grains are equiaxed α. On SEM magnification, the specks in the parent metal appear as swarfs probably due to polishing. Note absence of cracking (× 100).

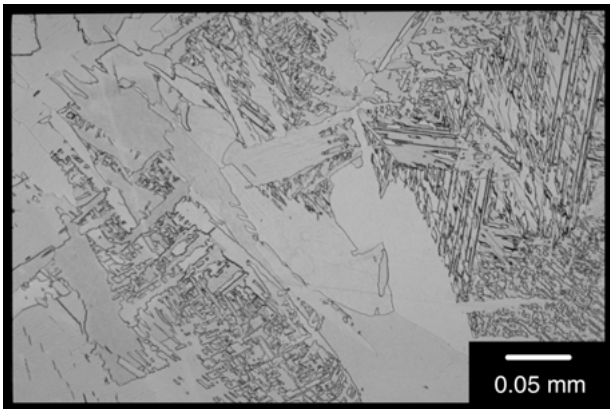

Figure 6 GTAW joint, abundance of Widmanstätten structures. The HAZ extended up to 15 mm of each side of the joints (× 200).

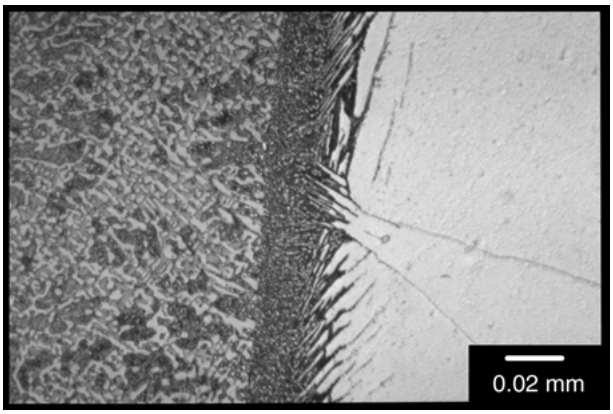

Figure 7 Typical Ti–15Cu–25Ni brazing. Filler alloy is heavily segregated. Presence of Widmanstätten lamellae and intermetallic compounds in the interdiffusion zone (× 500).

Microstructure. Figs 4–8 present typical patterns of the surfaces obtained. The native metal was made of grains that were fairly equiaxed and homogeneous. Annealing the machined specimens at 950 °C had little if no effect on grain structure (Fig. 4). Laser welding (Fig. 5) produced joint structures that were nearly identical to – and in continuity with the parent metal. The joints were devoid of visible contamination and no Widmanstätten structures were present.

In contrast to laser joints, electric arc welding produced major alterations in the structure. The heating regimen associated with this technique converted the

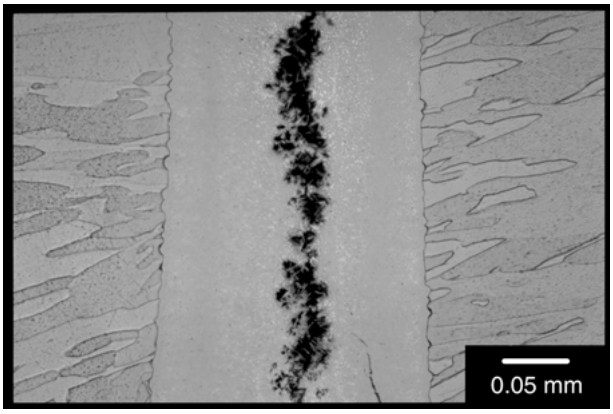

Figure 8 Typical Au–10.5Ag–7.5Pt-2Zn brazing. Well defined interface with substrate metal. Segregation in midportion of filler (× 200).

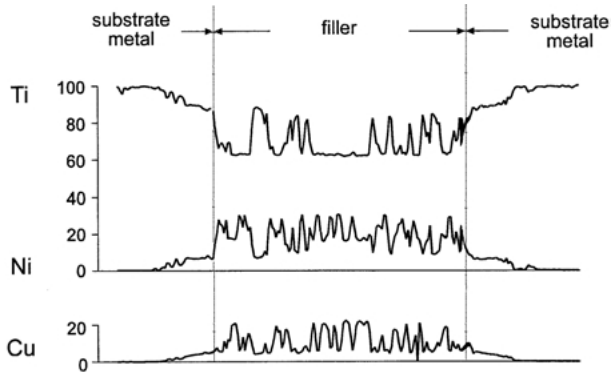

Figure 9 Elemental analysis Ti–15Cu–25Ni brazing. Note diffusion to and from the substrate metal (compare to Fig. 7).

initially granular parent metal to the acicular structure shown in Fig. 6. The Widmanstätten structures observed were present up to 15 mm away from the joints.

A representative TiCuNi joint is shown in Fig. 7. Here also, the heat generated during the fusion process induced changes in the grain structure of the substrate metal. Inside the joint, the brazing alloy segregated into intermetallic compounds and produced dendritic structures. The margins of the joints consisted of a layer of Widmanstätten lamellae that penetrated between the grains of the adjacent substrate metal.

Fig. 8 typifies our observations on gold brazings. While the interfaces with the substrate metal were well defined, segregation was observed in the mid-portions of the joints. This technique also altered the structure of the substrate metal.

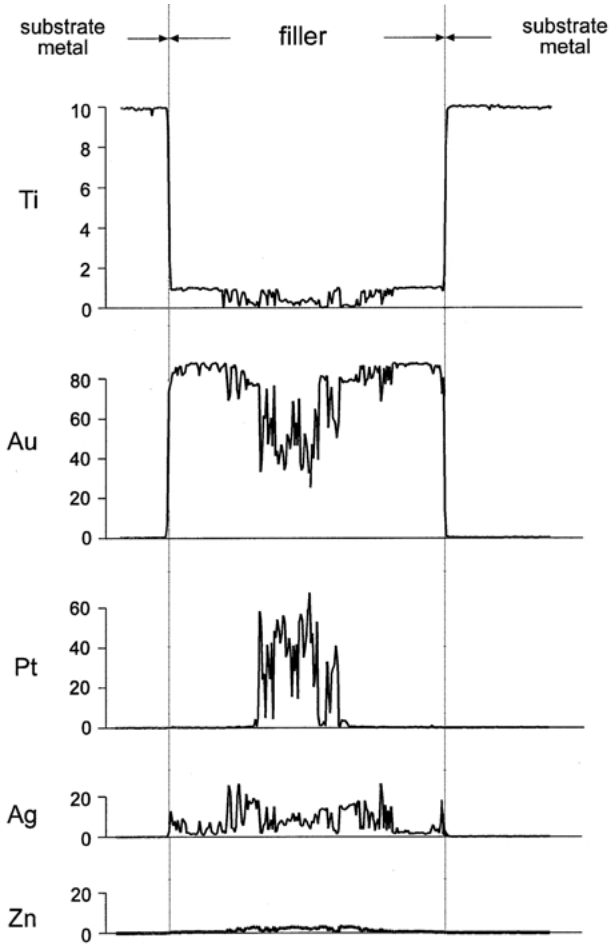

Figure 10 Elemental analysis of Microprobe Au–10.5Ag–7.5Pt–2Zn brazing. Note diffusion of Ti into the filler alloy and concentration of Pt in midportion of the joint (compare to Fig. 8).

Elemental analyzes. Results of the microprobe analyzes are presented in Figs 9 and 10. For both the TiCuNi and the gold-based brazing alloys, Ti was found to readily diffuse into the joint while Cu and Ni tended to spread into the marginal zones of the substrate metal. In the gold-based solder, the Pt concentrated into the middle third of the joint, while the proportion of Au increased in the zones close to the substrate metal. For both filler alloys, the microprobe tracings and microstructural analyzes were fully compatible.

Hardness. The substrate metals' hardness was 192 ± 8.3 Hv. Laser welding increased the joint's hardness to 267 ± 29.6 Hv and GTAW to 328 ± 17.9 Hv.

4. Discussion

4.1. Mechanical strength

The conditions of a monotonic uniaxial stress as in standard UTS tests bear little resemblance with the complex force vectors applied to prosthodontic structures in the oral environment. Indeed, during function, dental restorations are continuously subjected to courses of alternating stress vectors due to the sideways movements of the mandible during comminution of foodstuffs [21].

The UTS tests reported here were thus mainly performed for normative purposes. In this respect, three aspects should be pointed out: (1) On testing, the annealed substrate alloy presented a 68% higher UTS value than the ASTM F 67–83 specification for CpTi grade. The origin of this discrepancy is not known. (2) However, in a previous report [22] on ASTM B-265 grade 5 and B265–58T grade 2 (two CpTi's whose composition is close to the one used in the present study), the UTS of standard ASW 252 specimens was charted at 474–479 MPa – a value that lies within 5% of the tensile strength of our specimens. (3) The poor standing of gold brazings on Ti substrates concurs with data published by Lüthy *et al*. [23] using similar filler alloys.

With respect to clinical significance, however, more weight should be attributed to the data gathered under cyclic loading. In this respect, first, the CpTi compares favorably with the resistance of the conventional Au–Pd alloy tested previously [6] (333 vs. 340 MPa), thus implying that CpTi structures should perform adequately under functional stresses. Second, although GTAW yield UTS's that were superior to the substrate metal, their resistance to cyclic load application was more than 30% less than the substrate. Third, none of the gold-brazed specimens sustained an applied stress of 25 MPa up to 10^6 cycles.

4.2. Microstructure

Our micrographs of the fusion zone of laser welds showed equiaxed α grains, no cracks and a minor HAZ. The structure observed is at variance with data published by Denney and Metzbower on laser welds of CpTi. Their microstructures were heavily serrated and acicular α [22]

but no cracks were detected. In the latter study, however, a 13 kW CO_2 device was used while in the present tests, a Nd : YAG laser was operated at energy levels of maximum 3 kW. It would thus appear that the energy levels needed for industrial applications (i.e. large specimens and profound penetration) tend to locally ''overdose'' and produce deviant structures [24]. For instance, in a study by Lundquist (1995), welding of CpTi with a pulsed 90 W average Nd : YAG laser produced sound welds without porosity or cracks [25].

Titanium weldability decreases with increased levels of β stabilizers. In alloyed Ti, a number of authors have reported the occurrence of internal flaws which they associated with a loss of ductility through the development of transformation stresses due to a β-α lattice incompatibility [26]. Also, some investigators found a relation between the microstructure and the development of subsolidus weld cracks. Ti–6Al–4V for instance was far less susceptible to cracking than Ti–6Al–2Nb–1Ta–0.8Mo [27]. Large cracks were also observed in the β alloy Ti–15V–3Al–3Cr–3Sn [28].

There were no fissures in any of the joints tested. Yet, in our previous study on Au–Pd alloy [6], laser welding totally disrupted the alloy's normal granular structure and large cracks formed in the HAZ. The absence of cracks in the present study cannot be primarily attributed to differences in primary hardness or ductility of the parent metals since both are within the same order of magnitude. Indeed, according to the manufacturer, the AuPd alloy's hardness was 230–280 Hv (vs. 192 Hv for the Ti in our study).

The present data clearly show the dependency of substrate metal grain growth on the quantity of heat application. The effect is minor in laser welds, augmented in brazings and substantial in GTAW. Further, during the pilot tests for this study, some specimens were welded using a 30 kW high vacuum (5×10^{-5} Torr) electron beam welder. A specimen is shown in Fig. 11. The grains have grown to encompass the whole diameter of the specimens.

We made no efforts to specifically control cooling. Our experiment was merely designed to duplicate standard dental laboratory practices. However, it should be remembered that decreasing the cooling rate raises the β–α transition temperature and increases the volume percent of Widmanstätten structure [26].

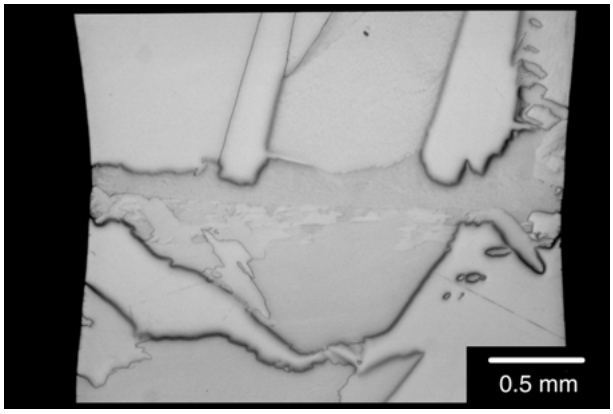

Figure 11 Low magnification of electron-beam welding (× 32). Note considerable increase in grain size.

4.3. Filler metals

Historically, Ag- and Al-based alloys were considered suitable filler metals for brazing titanium materials [29, 30]. However, their mechanical and galvanic properties were too dissimilar from the titanium substrate. During later developments, it was found that Ti-based filler metals presented superior characteristics as to their strength and resistance to corrosion and hence gained wide acceptance in industrial applications [31, 32].

However, the melting range of theses fillers is 902–932 °C and thus higher than the α–β transition temperature of CpTi. This relation is considered detrimental by some [33] and the addition of Zr to the Ti–Cu–Ni alloy was proposed to decrease the melting range to the lower 800s [34]. Although this parameter was not investigated specifically, no detrimental effect related to the β–α transition could be determined in our study. Indeed, in spite of the presence of a HAZ at the filler-substrate interface, the resistance to cyclic loading of Ti–Cu–Ni brazings was superior to the most resistant joints on the Au–Pd substrate previously tested [6].

The interdiffusion zone between the substrate metal and the filler has been described by others [35]. Cu and Ni are known β stabilizers. During brazing, copper and nickel atoms diffuse from the liquid filler metal into the original equiaxed α which transforms into β phase. On cooling the β phase transforms into lamellar α and β Widmanstätten structure. The intermetallic phases Ti_2Cu and Ti_2Ni also form during this process (Fig. 7).

Nickel was part of the Ti-based filler metal used in the present study and also is also included in the Ag–Cu–Ni–Li system, another common filler for titanium brazings. Yet due to its allergenic potential [36], Ni is being progressively banned from biomedical applications. It is generally accepted that future strong and corrosion-resistant filler alloys for Ti brazing should thus be devoid of Ni and alternative elements must be found. In this respect, the Ti–Cu–Pd, Au–Ag–Cu–Zn and Au–Ag–Pd–Cu–In–Zn systems used in Lüthy *et al*.'s report [23] may deserve further investigation. However, whether nickel in the oral environment actually produces the damaging effects many authors fear is questionable in light of recent reports on the long-term follow-up of a 66% Ni alloy for fixed prostheses [37]. As to the gold-based brazings, their poor standing under fatigue loading precludes any clinical application.

4.4. Mechanical resistance and microstructure

The findings herein do not allow major conclusions as to the influence of microstructure on mechanical resistance [38]. Indeed, our data are conflictual in that no microstructural alteration could be correlated with the fatigue resistance observed (again, the resistance to fatigue loading being considered superior in its validating potential relative to UTS tests). The Ti–Cu–Ni brazings were heavily segregated and structurally inhomogeneous, yet these joints were the strongest. Conversely, laser welds presented regular micostructures with equiaxial grains, no cracking or voids and their fatigue resistance was lower than the brazings. Last, electric arch welding produced joints with a highly

acicular structure. These joints were superior to the native substrate under monotonic tensile load but ranged last when subjected to fatigue stresses. A similar observation was made in our previous study on Au–Pd joints [6]. In the latter instance, the laser-welded joints were highly dendritic and their UTS was highest (633 MPa). Their fatigue resistance, however, was in the lower range of the joints tested (174 MPa).

As to the elemental analysis performed, the tracings are just the opposite of our findings on AuPd alloy. The filler that diffused most inside the substrate metal also yield the strongest joints under fatigue loading.

Judging from the small microstructural differences between our native and annealed substrate, our annealing process was actually a stress relief rather than a recrystallisation. Our data showed an improvement in fatigue resistance (312→340 MPa) with annealing. By contrast, Morita *et al*. found a significant decrease (350→200 MPa) when testing cold rolled and recrystallized states [39]. While their substrate alloy was very similar to ours, there was a striking difference in microstructure between both states. As to the absolute values obtained, the 30% difference with our data is not explained. Further, transformed structures such as Widmannstätten lamellae have been shown to increase toughness [13], they will, however, hamper formability of the metal [40, 41].

5. Conclusions

1. Under fatigue stress application, the titanium-based brazings as well as the laser- and electric arc welds performed equally well if not better than a previously tested AuPd alloy, thus indicating clinical applicability.

2. There was a definite increase in grain size with increased heat application.

3. No feature of the microstructures observed or the elemental analysis could be correlated with the specimen's resistance to fatigue stress application.

References

1. STEINEMANN, P. A. MÄUSLI, S. SZMUKLER-MONCLER, M. SEMLITSCH, O. POHLER, H. E. HINTERMANN and S. M. PERREN, in ''Titanium 92', Science and Technology'', edited by F.H. Froes and I. Caplan (The Minerals, Metals and Materials Society, 1993) p. 2689.
2. P. I. BRÅNEMARK, R. ADELL, U. BREINE, B. O. HANSSON, J. LINDSTRÖM and A. OHLSSON, *Scand. J. Plast. Reconstr. Surg*. **3** (1969) 81.
3. D. F. WILLIAMS, in ''Biocompatibility of Clinical Implant Materials'', edited by D.F. Williams (CRC Press, Boca Raton, FL 1984) p. 44.
4. American Society for Metals. ''Metals Handbook – Desk Edition'' (ASM International, Materials Park, OH, 1998) p. 555.
5. J. E. LEMONS, L. C. LUCAS and B. JOHANSSON, *Implant. Dent*. **1** (1992) 107.
6. H. W. A. WISKOTT, F. MACHERET, F. BUSSY and U. C. BELSER, *J. Prosthet. Dent*. **77** (1997) 607.
7. H. W. A. WISKOTT, F. MACHERET, C. SUSZ, R. BARRAUD, L. HAENNY and J. M. MEYER, *J. Fra. Biomat. Dent*. **11** (1996) 101.
8. G. SJÖGREN, M. ANDERSON and M. BERGMAN, *Acta. Odontol. Scand*. **46** (1988) 247.
9. E. BERG, W. C. WAGNER, G. DAVIK and E. R. DOOTZ, *J. Prosthet. Dent*. **74** (1995) 250.
10. R. R. WANG and C. T. CHANG, *ibid*. **79** (1998) 335.
11. T. FORSMAN, in ''Proceedings of the 6th Nordic Laser Materials Processing Conference (NOLAMP 6), Luleå, Sweden, August 27–29, 1997'', edited by C. Magnusson and H. Engström (Materials Processing Division, Luleå University of Technology 1998) p. 44.
12. American Society for Testing and Materials. ''Unalloyed titanium for surgical implant applications''. Annual Book of ASTM Standards, specification F67–83, v. 13.01 (ASTM, Philadelphia, PA, 1984).
13. American Society for Metals. ''Metals Handbook'' v. 19 (ASM International, Materials Park, OH, 1996) p. 830.
14. C. A. BLUE and R. Y. LIN, *Process Adv. Mater*. **4** (1994) 21.
15. E. J. HEARN, in ''Mechanics of Materials'' (Pergamon Press, Oxford, 1985) p. 811.
16. H. W. A. WISKOTT, J. I. NICHOLLS and U. BELSER, *Dent. Mater*. **10** (1994) 215.
17. H. W. A. WISKOTT, J. I. NICHOLLS and U. BELSER, *Int. J. Prosthodont*. **8** (1995) 105.
18. E. P. POPOV, in ''Introduction to the Mechanics of Solids'' (Prentice Hall, Englewood Cliffs, NJ 1968).
19. W. J. DIXON and A. M. MOOD, *J. Amer. Stat. Assn*. **43** (1948) 109.
20. H. W. A. WISKOTT, J. I. NICHOLLS and U. BELSER, *Int. J. Prosthodont*. **9** (1996) 117.
21. H. GRAF and A. W. GEERING, *Oral Sci. Reviews*. **10** (1977) 1.
22. P. E. DENNEY and E. A. METZBOWER, *Welding Res. Suppl*. **68** (1989) 342-s.
23. H. LÜTHY, J. M. MEYER, O. LOEFFEL and P. SCHÄRER, *Quintessenz Zahntech*. **21** (1995) 627.
24. H. MOURTON and S. K. MARYA *Int. J. Join Mater*. **6** (1994) 100.
25. A. LUNDQUIST, in ''Welding of superalloys with Nd:YAG laser''. MS thesis. Luleå University of Technology (1995).
26. B. K. DAMKROGER, G. R. EDWARDS and B. B. BATH, *Welding Res. Suppl*. **68** (1989) 290-s.
27. D. HAYDUK, B. K. DAMKROGER, G. R. EDWARDS and D. OLSON, *Welding J*. **65** (1986) 251-s.
28. H. INOUE and T. OGAWA. *Welding Res. Suppl*. **74** (1995) 21-s.
29. W. T. KAARLELA and W. S. MARGOLIS, *Welding J*. **53** (1974) 629.
30. X. HEBERARD, *Titanium*. **80** (1980) 2415.
31. D. G. HOWDEN and R. W. MONROE, *Welding J*. **51** (1972) 31.
32. S. W. LAN, *ibid*. **61** (1982) 23.
33. T. ONZAWA, A. SUZUMURA and M. W. KO, *Welding Res. Suppl*. **70** (1990) 462-s.
34. E. LUGSCHEIDER and U. BROICH, *ibid*. **70** (1990) 169-s.
35. E. CHANG and C. H. CHEN, *J. Mater. Engng. Perform*. **6** (1997) 797.
36. A. SCHNUCH, J. GEIER, W. UTER, P. J. FROSCH, W. LEHMACHER, W. ABERER, M. AGATHOS, R. ARNOLD, T. FUCHS, B. LAUBSTEIN, G. LISCHKA, P. M. PIETRZYK, J. RAKOSKI, G. RICHTER and F. RUEFF, *Contact Dermatitis*. **37** (1997) 200.
37. E. SPIECHOWICZ, P. O. GLANTZ, T. AXELL and P. GROCHOWSKI, *Eur. J. Prosthodont. Rest. Dent*. **7** (1999) 41.
38. J. SINGH J, *J. Mater. Sci*. **29** (1994) 5232.
39. F. MORITA, J. TAKAHASHI, S. MUNEKI and T. KAINUMA, in ''Proceedings of the TMS annual meeting'' (San Antonio, Tx, 16–19 February 1998) p. 29.
40. S. GUILLARD, M. THIRUKKONDA and P. K. CHAUDHURY, in ''Proceedings of the TMS annual meeting'' (Anaheim, CA, 5–8 February 1996) p. 93.
41. K. W. BOENING, M. H. WALTER and P. D. REPPEL, *J. Oral Rehabil*. **19** (1992) 281.

Received 7 February
and accepted 25 October 2000